The Presence of Linear Wavelike Modes in a Zonally Symmetric Model of the Tropical Atmosphere

JOHN R. ANDERSON* AND DUANE E. STEVENS

Department of Atmospheric Science, Colorado State University, Fort Collins, CO 80523

(Manuscript received 14 April 1986, in final form 3 February 1987)

ABSTRACT

The linear, zonally symmetric modes of the basic state of a Hadley cell are examined. We find that the inclusion of the divergent basic state leads to the formation of a new class of slowly oscillating modes, some of which have periods in the range of 40–50 days. The modes have many features in common with the observed tropical 40–50-day oscillation; however, an explanation for the observed fluctuations in convective cloudiness remains a topic for future work.

1. Introduction

The existence of a quasi-periodic oscillation with a period of 40–50 days was discovered by Madden and Julian (1971) in time series of tropical surface pressure and zonal wind. Since that time, various investigators have become aware of the presence of this fluctuation in most tropical atmospheric variables including winds, surface pressures and convective cloudiness. The presumed energy source for this motion seems to lie in the fluctuations of latent heating associated with deep convection. This variation of the convective heating has been directly observed by Yasunari (1980) and Julian and Madden (1981), as well as several more recent investigators.

In order to test the hypothesis that the tropical motions are being driven by the changes in convective heating, we have performed a linear-forced calculation where the heating had a prescribed spatial distribution and oscillation period. The results of this calculation appear in Anderson (1984) and Anderson and Stevens (1987), where the response of several different linear models including one with a "Hadley cell" basic state and cumulus friction effects are presented. These calculations indicate that the most complete of the linear models was able to reproduce many aspects of the observed motions; however, this sort of calculation cannot provide an explanation for the selection of the 40–50 day time scale.

The first suggestion of a possible source for the oscillation time scale resulted from a linear wave calculation performed by Chang (1977), which included the effects of dissipation such as might be expected from cumulus momentum transport. Chang undertook the calculation as an attempt to understand the apparently inconsistent, deep, vertical structure and slow eastward propagation speed of the observed zonal wavenumber 1 oscillation. When the effects of the added dissipation and the Doppler shifting of the wave frequency by the mean zonal wind were included, Chang was able to obtain a propagation speed compatible with the observed motions.

Anderson et al. (1984) performed an observational diagnostic calculation which was designed to determine if the period of the motion could result from the resonant excitation of the viscous equatorial Kelvin wave modes reported by Chang. They reasoned that if the oscillation time scale resulted from a resonant excitation of the Chang mode, then one ought to see a seasonal change in the oscillation freuqency as the zonal winds responsible for the Doppler shift effects underwent their seasonal changes. A climatology of the oscillation frequency based on West Pacific wind data failed to show the seasonal effects; the observed oscillation period did undergo changes over a fairly large range (35–55 days) in an apparently random fashion, but the seasonal climatology of the period was found to lie between 43 and 45 days throughout the year. In spite of the failure of this mechanism to explain the time scale, the more complex linear numerical calculations just mentioned do show that the mechanism proposed by Chang does provide a reasonable representation of the deep tropical response to the thermal forcing.

In this paper we explore another possible source for the oscillation time scale. Here we will consider the behavior of steady state, thermal, wind modes in the context of a more complicated basic state instead of the traveling wave modes examined by Chang. In order to limit the computational complexity of the problem,

* Present affiliation: Department of Meteorology, University of Wisconsin, Madison WI 53706

we have limited ourselves to the simplest possible divergent basic state—namely, a zonally symmetric "Hadley" cell. We will show that for this simple case the steady state, zonally symmetric, thermal wind modes associated with a resting basic state become slowly oscillating modes, some of which have periods in the 40–50 day range.

We realize that neither the observed time mean state nor the 40–50 day fluctuations are purely zonally symmetric; however, an observational study by Anderson and Rosen (1983) has shown that a zonally symmetric part of the oscillation is present, so perhaps our approach here can be considered a suitable first approximation to calculations with more general divergent basic states.

2. Model equations and design

The model used for this work is a zonally symmetric primitive equation model defined with equatorial β-plane geometry. We have constructed two models for use in this calculation: a linear and a nonlinear one. The nonlinear model is used with prescribed forcing to define our Hadley cell basic state. This model is derived using the hydrostatic and anelastic approximations with physical height as the vertical coordinate. Using conventional meteorological notation, the zonally symmetric nonlinear system can be written as follows:

$$u_t = -(vu_y + wu_z) + \beta yv - \alpha(y,z)u + \mu u_{zz} + F_{cx} \quad (1)$$

$$v_t = -(vv_y + wv_z) - \beta yu - \frac{1}{\tilde{\rho}} p_y - \alpha(y,z)v + \mu v_{zz} + F_{cy} \quad (2)$$

$$\theta_t = -[v\theta_y + w(\theta + \tilde{\theta})_z] + Q - \gamma(y,z)\theta + \mu\theta_{zz} \quad (3)$$

$$-\frac{1}{\tilde{\rho}}(\tilde{\rho}w)_z = v_y \quad (4)$$

$$\left(\frac{p}{\tilde{\rho}}\right)_z = \frac{g}{\tilde{\theta}}\theta. \quad (5)$$

The variables $\tilde{\rho}, \tilde{\theta}, \tilde{p}$ represent the hydrostatic reference stratification, which depends only on height. The model includes three forms of dissipation. The first is a simple Newtonian cooling/Rayleigh friction term denoted by γ and α. These terms are used to represent surface friction and impose the model boundary sponges as described below; they are small in the interior. A second order diffusion term is included to simulate vertical mixing. Finally, a cumulus momentum transport parameterization is used following Schneider and Lindzen (1976) and Stevens and Lindzen (1978):

$$F_{cx} = \frac{1}{\tilde{\rho}}[M_c(u - u_c)]_z \quad (6)$$

$$F_{cy} = \frac{1}{\tilde{\rho}}[M_c(v - v_c)]_z \quad (7)$$

where u_c, and v_c are the winds at cloud base level and M_c, the cloud mass transport, is given by

$$M_c(y,z) = [M_c(y)] \begin{cases} 1 - \exp\left(\dfrac{p_t - \tilde{p}(z)}{p_{\text{dtr}}}\right), & p_t \le \tilde{p}(z) \le p_c \\ 0, & \text{otherwise.} \end{cases} \quad (8)$$

Here p_t is the pressure at cloud top and p_{dtr} is a detrainment scale which we take to be 75 mb.

In all cases the cumulus momentum transport effects and cumulus heating terms are linked by the requirement that the latent heat released by the cloud is equal to the latent heat represented by the amount of water vapor contained in the cloud mass flux at cloud base. The models are discretized using a second-order finite difference technique in the vertical, and a Fourier spectral representation in the horizontal. The model upper boundary is at 17 km and the upper 2 km of the model domain consist of a Newtonian cooling sponge designed to reduce spurious wave reflection. Complete descriptions of the Fourier discretization scheme and boundary sponges appear in Anderson and Stevens (1987). The model used here is identical to that one in all aspects, except for the horizontal and vertical resolution of the low-resolution calculations. The horizontal domain extends from 46°S to 46°N, with Rayleigh friction sponges occupying the regions poleward of 35° latitude. We have tested our numerical discretization technique and boundary treatment by comparing it with the analytical infinite β-plane results from Gill (1980) for forced shallow water problems, and have obtained essentially identical results.

The nonlinear solution is achieved by integrating the zonally symmetric version of the model to equilibrium starting from rest, using a prescribed thermal forcing that contains heating in the deep tropics and cooling in the subtropics and midlatitudes. A plot of the heating function is given in Fig. 1; the heating is assumed to be symmetric in the meridional direction about the equator. The model integration is performed using a trapezoidal semi-implicit time step, and is run until the system reaches a steady state solution. Plots showing the results of the basic state calculation are given as Fig. 2. This resultant Hadley circulation will be taken to be the base state for our linear model calculations. This plot of the basic state Hadley circulation is for the lower resolution domain (described later). A plot of Hadley cell for the higher-resolution case appears in Anderson and Stevens (1987).

Model calculations have been made for the results presented here with both 10 and 20 vertical levels and 10 and 20 meridional wavenumbers. The advantage of the low-resolution calculations is that the number of model degrees of freedom is small enough that the

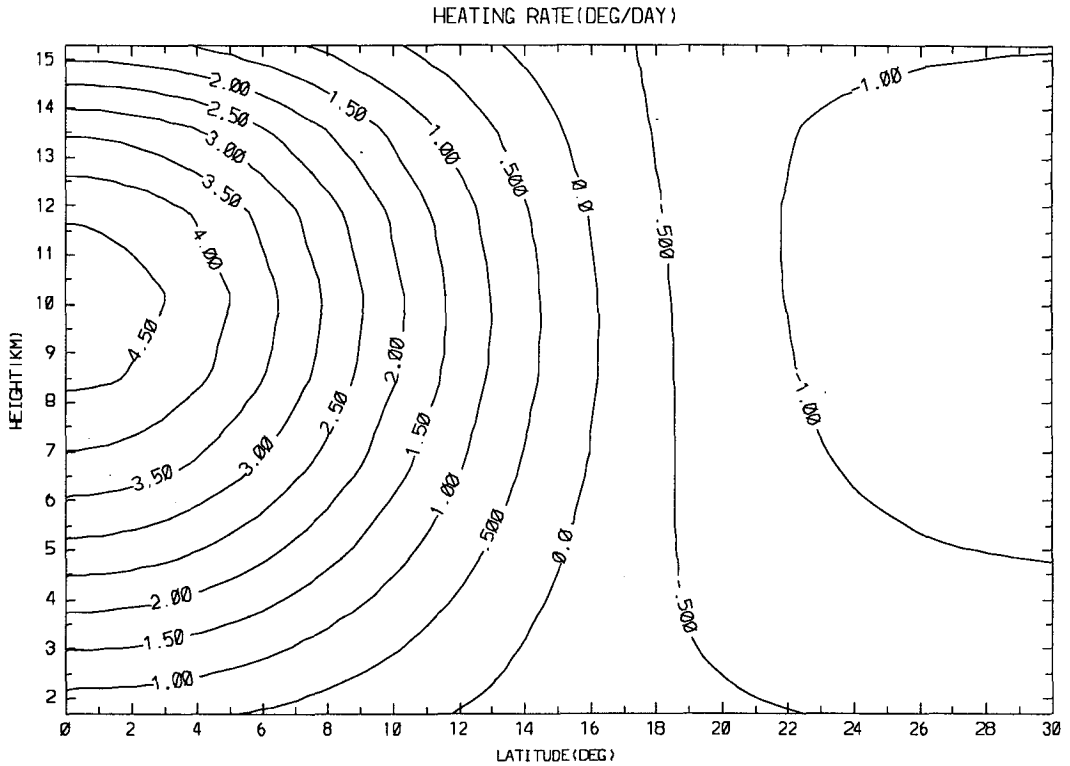

FIG. 1. Thermal forcing field (deg/day) for Hadley cell calculation.

normal modes of the system can actually be found using matrix eigenvalue techniques. The accuracy of the low-resolution runs is, however, somewhat suspect for small vertical-scale phenomena so we have also performed prognostic calculations with higher-resolution models to verify some of the solution properties.

The linear model is constructed by performing a conventional linearization of the original equations around our basic state Hadley circulation. This process yields the following prognostic system:

$$u'_t = -(\bar{v}u'_y + \bar{w}u'_z) + \beta y v' - \alpha(y,z)u' + \mu u'_{zz} + F'_{cx} - (v'\bar{u}_y + w'\bar{u}_z) \quad (9)$$

$$v'_t = -(\bar{v}v'_y + \bar{w}v'_z) - \beta y u' - \frac{1}{\tilde{\rho}}p'_y - \alpha(y,z)v' + \mu v'_{zz} + F'_{cy} - (v'\bar{v}_y + w'\bar{v}_z) \quad (10)$$

$$\theta'_t = -(\bar{v}\theta'_y + \bar{w}\theta'_z) + Q' - \gamma(y,z)\theta' + \mu\theta'_{zz} - [v'\bar{\theta}_y + w'(\bar{\theta}+\tilde{\theta})_z] \quad (11)$$

$$-\frac{1}{\tilde{\rho}}(\tilde{\rho}w')_z = v'_y \quad (12)$$

$$\left(\frac{p'}{\tilde{\rho}}\right)_z = \frac{g}{\tilde{\theta}}\theta' \quad (13)$$

where

$$F'_{cx} = \frac{1}{\tilde{\rho}}\{[\bar{M}_c(u'-u'_c)]_z + [M'_c(\bar{u}-\bar{u}_c)]_z\} \quad (14)$$

and

$$F'_{cy} = \frac{1}{\tilde{\rho}}\{[\bar{M}_c(v'-v'_c)]_z + [M'_c(\bar{v}-\bar{v}_c)]_z\}. \quad (15)$$

This system is essentially equivalent to that used by Rosenlof et al. (1986).

3. Linear eigenmode calculations

If we provide a suitable linear closure for Q' and M'_c in the linear system we can then write the linear problem in schematic matrix form as $\partial \mathbf{S}/\partial t = \mathbf{AS}$. Here $\mathbf{S}$ is the model state vector containing the u, v, and θ amplitudes for each spatial degree of freedom, and $\mathbf{A}$ is a matrix which describes the dynamical processes contained in the linearized governing equations. The matrix $\mathbf{A}$ is determined using the "single time step" technique described by Hoskins and Karoly (1981). This method consists of using a transform procedure to calculate the elements for each column of $\mathbf{A}$. To do this, we compute the time derivatives which would result from a perturbation state consisting of zero, except for the state variable represented by the column which is given a value of one. For our low-resolution zonally

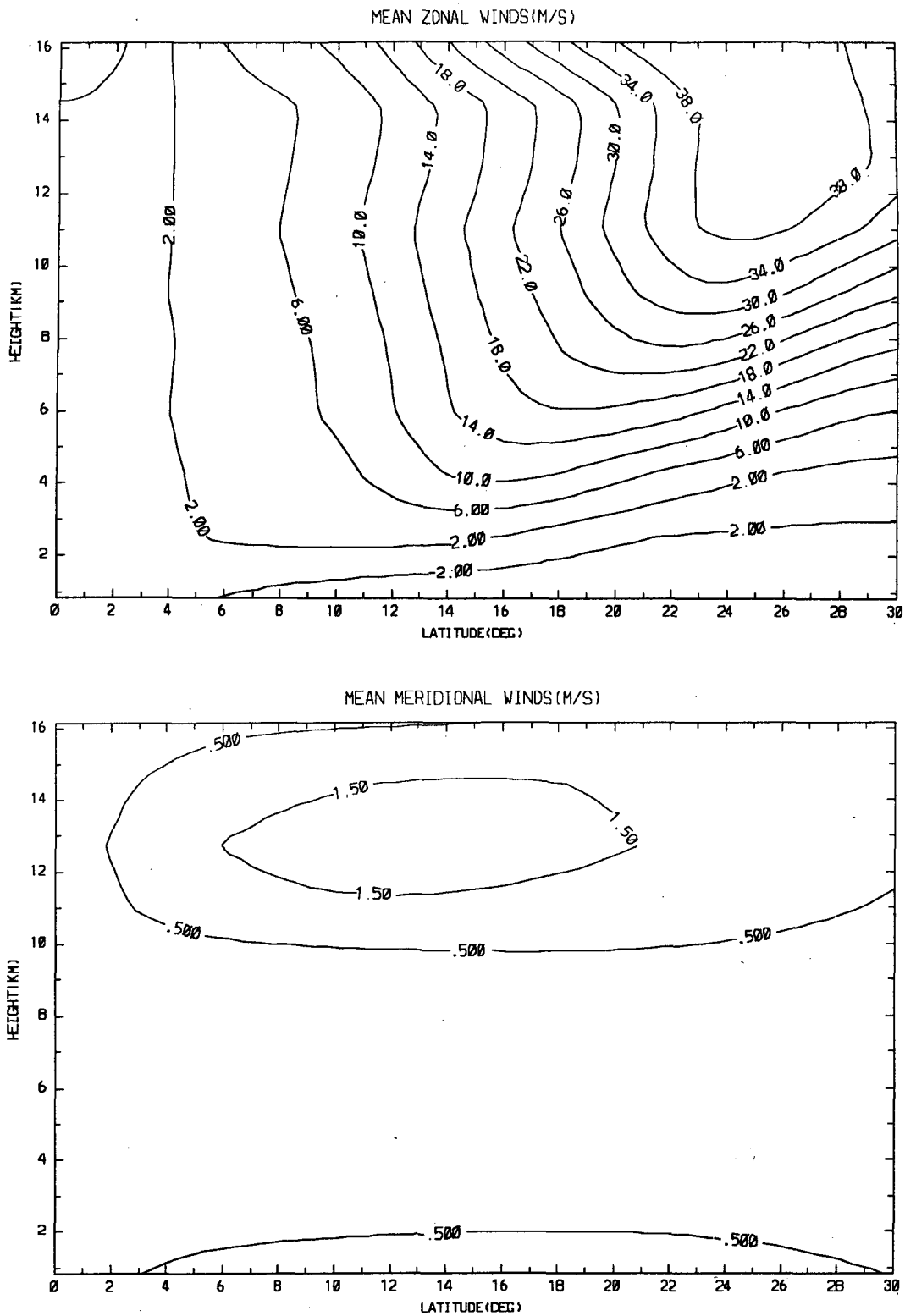

FIG. 2. Zonally symmetric Hadley cell resulting from the nonlinear calculation.

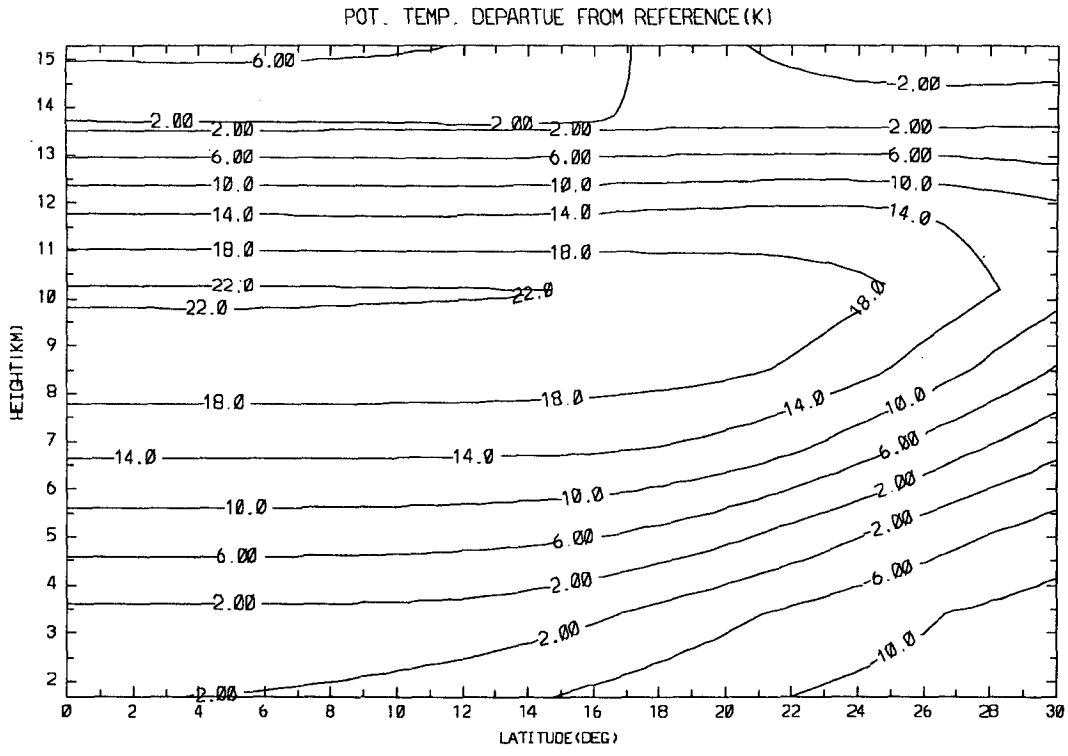

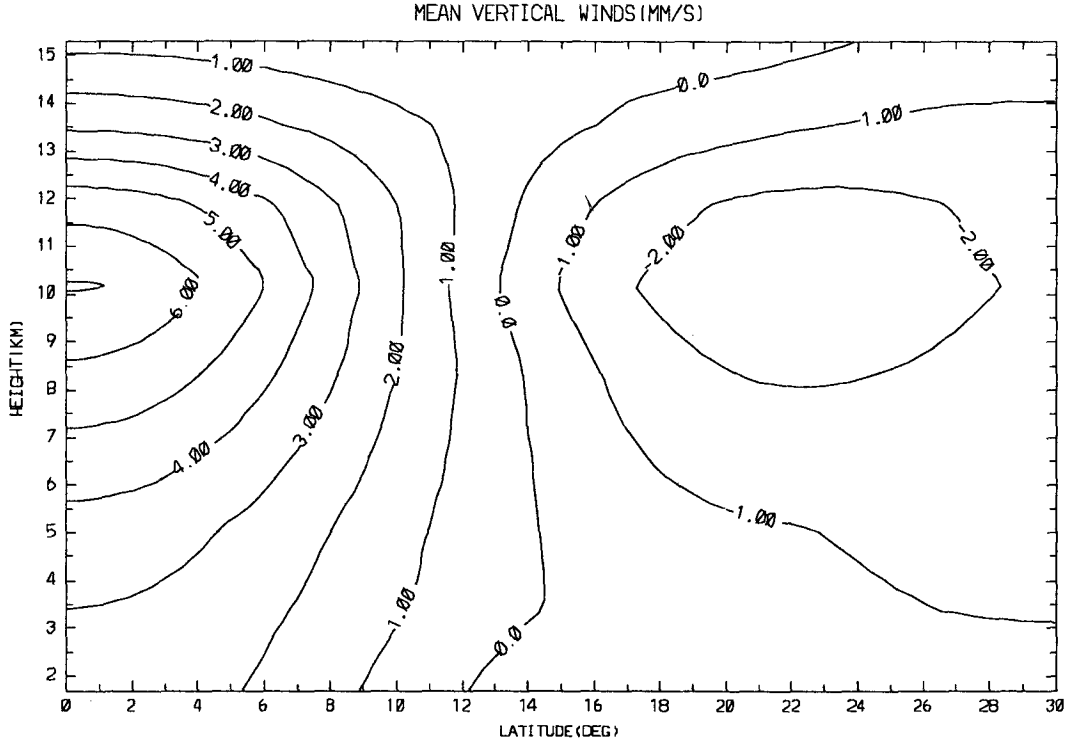

FIG. 2. (*Continued*)

symmetric model with 10 vertical levels and 10 (complex) meridional wavenumbers, **A** is a real 600 by 600 matrix. The time dependent solutions of this matrix problem all have the following form:

$$\mathbf{S}(t) = \sum_{i=1}^{N} a_i \mathbf{E}_i \exp(\lambda_i t),$$

where the λ_i are the eigenvalues of **A** and the $\mathbf{E}_i$ are the associated eigenvectors. The eigenmode amplitudes a_i are determined from the initial conditions. The eigenvalues and eigenvectors of **A** were found using standard EISPACK routines and 64-bit precision. In every case presented here, the routines reported acceptable solution accuracy.

For the case of the infinite equatorial β-plane geometry with no dissipation, no heating, and a resting basic state, the matrix problem is subject to significant simplification, and analytic solutions are known. The solutions, which are described in Lindzen (1967) and Matsuno (1966), are found by first performing a separation of variables in the vertical to derive a set of "equivalent shallow water" equations for each vertical wave mode with the "equivalent depth" separation constant representing the vertical scale of each mode. The shallow water system can be rewritten as a classical eigenvalue problem which has known solutions. In general, each vertical mode gives rise to a family of slow Rossby wave modes and two sets of inertia-gravity modes. The equatorial Kelvin wave exists as a special case of this solution. When only the zonally symmetric ($k = 0$) modes are considered, the Kelvin and Rossby modes collapse into a degenerate set with exactly zero frequency. This is representative of the ability of any motion in thermal wind balance to be a steady solution of the resting zonally symmetric problem. The inertia-gravity waves are still present and remain a fast-oscillating feature.

A scatter plot of the eigenvalues for our linear model with a resting basic state and no cumulus heating or cumulus friction is shown in Fig. 3. Here, each point on the plot is one complex eigenvalue λ_i which has both an oscillation frequency and a growth/damping time scale. On this plot, slowly oscillating modes are found on the left and modes which oscillate faster are found on the right. All of the modes for this case are stable (damped) and are so identified in the plot with a minus sign. Modes near the top (bottom) of the plot damp quickly (slowly). Due to the logarithmic nature of the plot time scale, it is not possible to show modes at zero frequency; therefore, all modes with frequencies slower than 2×10^{-7} sec (period approximately 1 yr) are plotted at this frequency. It can be seen that the performance of our model is very similar to the analytic solution, in that there is a set of nonoscillating modes in thermal wind balance and a set of fast oscillating

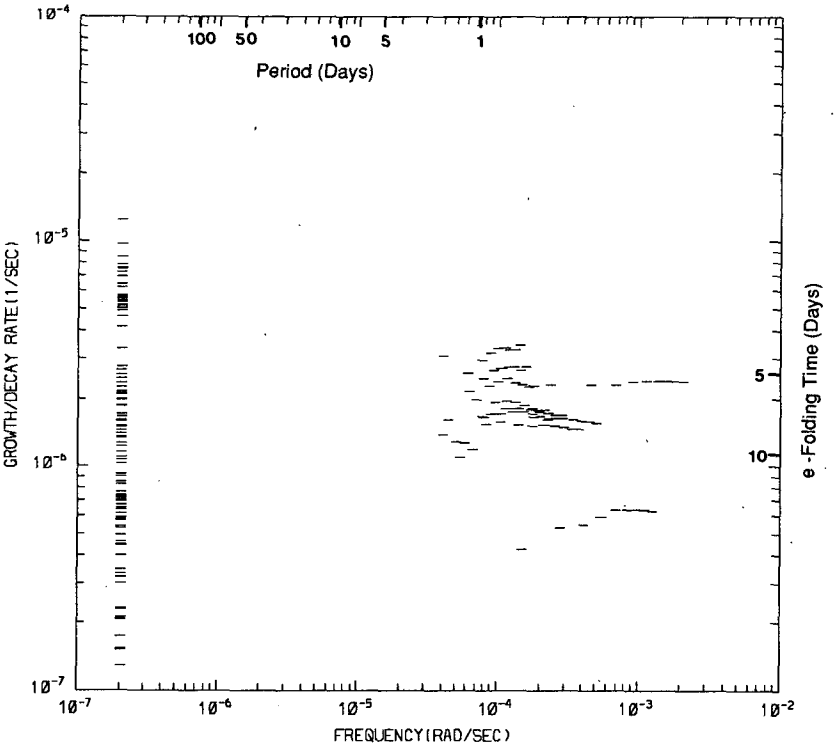

FIG. 3. Model eigenvalues for resting basic state. Modes with frequencies $< 2 \times 10^{-7}$ sec are plotted at 2×10^{-7} sec.

gravity modes. The various damping times associated with the modes are due to the damped boundary treatment in the model, which causes all of the modes to decay at least to some extent. The damping also removes the degeneracy of the slow modes.

The next case which we will consider includes the Hadley cell basic state shown in Fig. 2. For this calculation we have not included the direct effects of the basic state cumulus mass transport, nor have we included any perturbation clouds, so we will take $Q' = Mc' = 0$. The results from this calculation are shown in Fig. 4, and have a decidedly different character from that of the resting basic state. One change in the solution is the rearrangement of the inertia–gravity modes due to the inclusion of the zonal wind field and the resultant change in inertial stability. A second and extremely interesting effect is the appearance of low-frequency oscillating modes with periods in the 20–100 day range. We have examined the structure of the modes in this time scale which exhibit the longest decay time and would thus presumably have the largest amplitude response to random forcing. The u-wind structure of three of these modes, which are labeled a, b, and c in Fig. 4, are given in Fig. 5. In each case the modes are very nearly in thermal wind balance with extremely small v-wind fields. The dynamics of the oscillation is dominated by the advection of both perturbation u-wind and temperature fields due to the basic state divergent circulation. Our interpretation of these results is that the model modes are not individually significant but that they represent the continuum response of the real continuous atmosphere, which appears as a set of discrete modes in our model due to the finite number of degrees of freedom in the model. These time-dependent motions are the result of modifying the stationary thermal wind solutions by the inclusion of the background Hadley circulation. These structures are similar to the structure of the observed zonally symmetric oscillation as reported by Anderson and Rosen (1983).

The resulting complex eigenvalues from a similar calculation which differ only by the inclusion of the basic state cumulus mixing parameterization are presented in Fig. 6. These results are similar in character to that presented before; however, all of the modes appear to be somewhat more damped.

4. Linear prognostic calculations

We have chosen to employ a linear prognostic model for the purpose of verifying our eigenmode solutions at somewhat higher resolution. The results of this section were calculated using 20 vertical levels and 20 meridional wavenumbers on our domain. In the prognostic calculation we integrate the model forward in time, starting with a basic state which contains spatially random perturbations in temperature. Due to the linear nature of the problem, any linear combination of

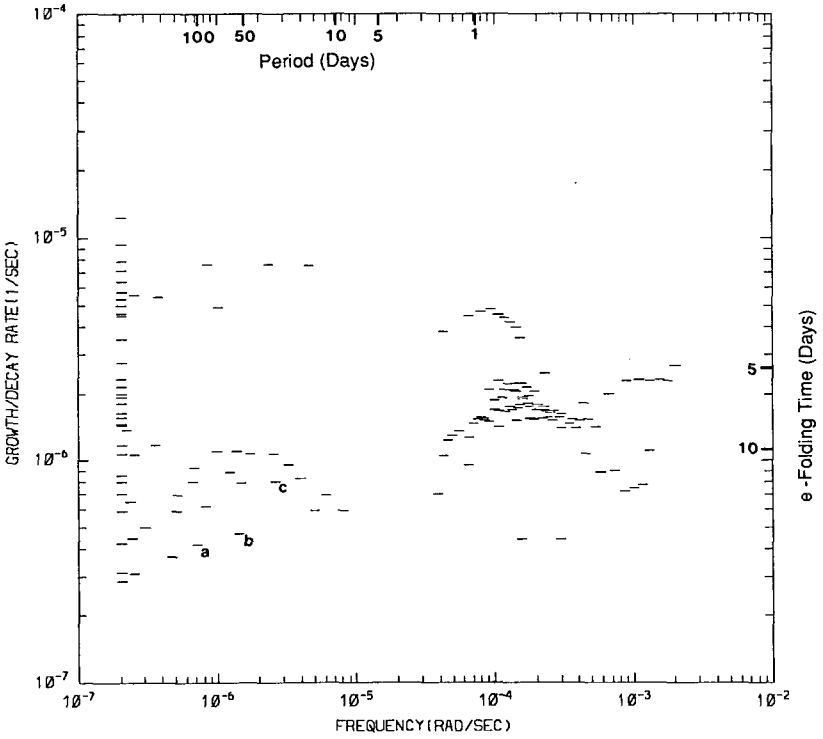

FIG. 4. Model eigenvalues for Hadley cell basic state and no basic state cumulus mixing.

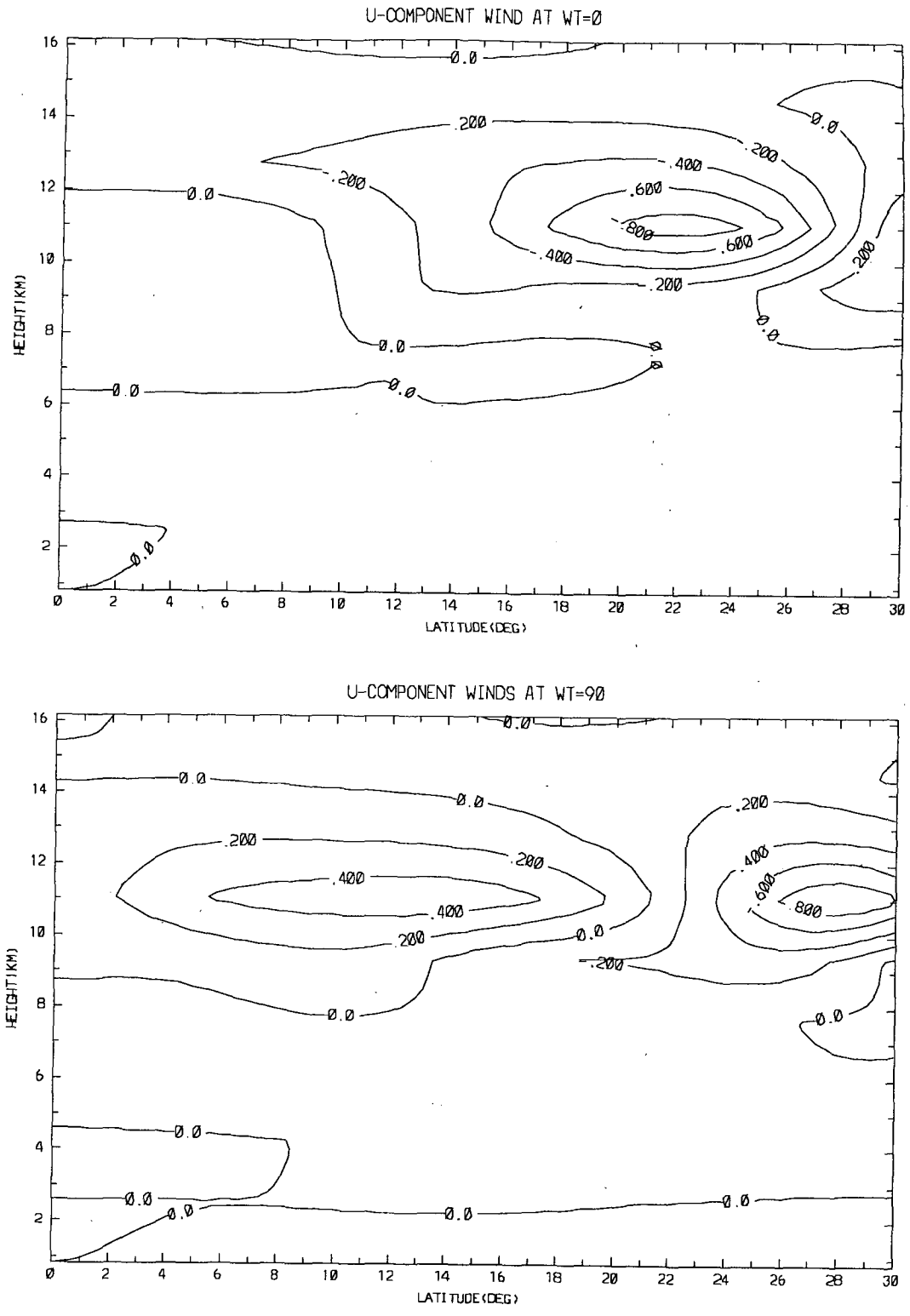

FIG. 5a. *U*-wind field of eigenmode at phase 0 and $\pi/2$. Mode depicted is associated with eigenvalue labeled (a) on Fig. 4.

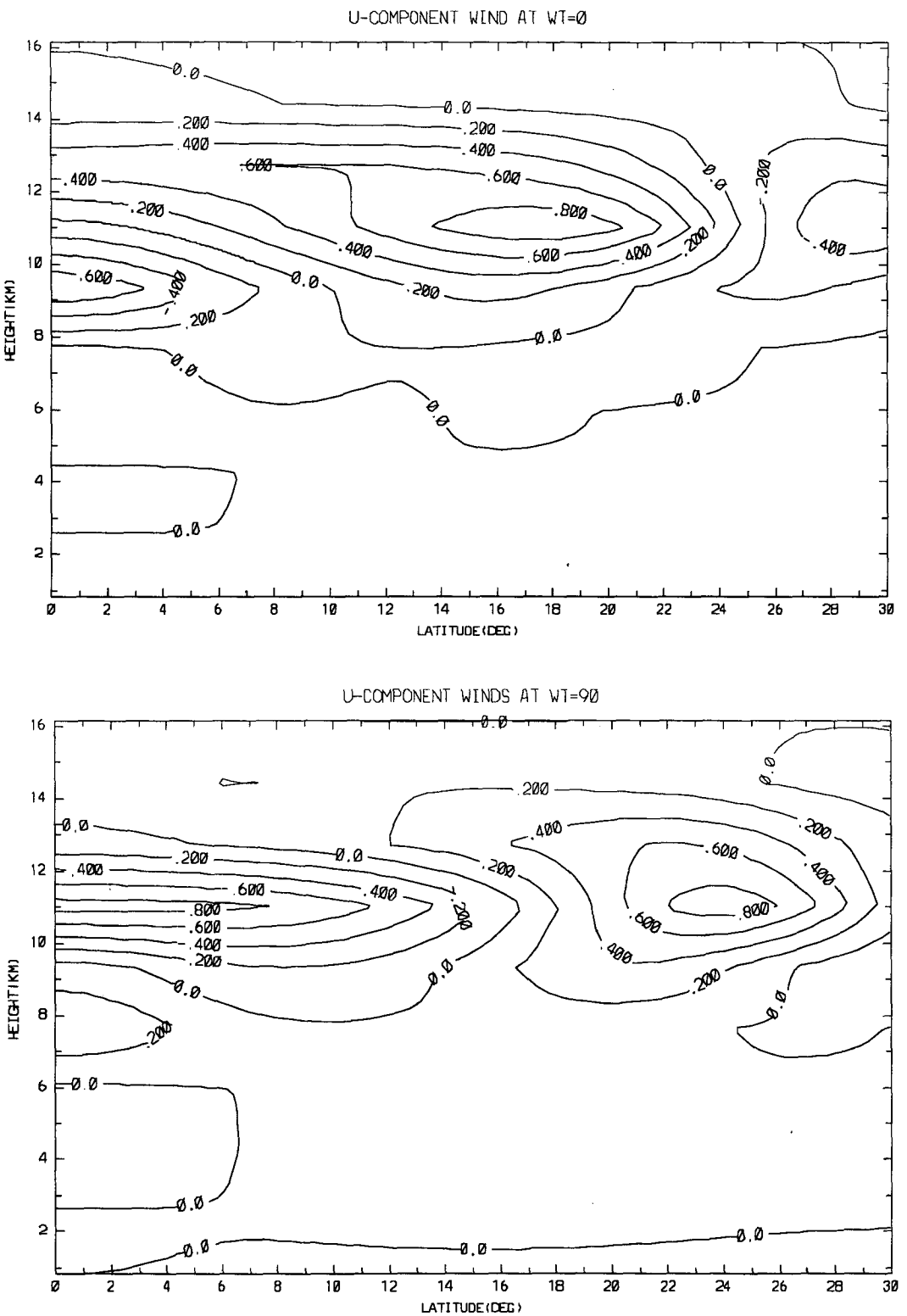

FIG. 5b. As in Fig. 5a, but mode depicted is associated with eigenvalue labeled (b) on Fig. 4.

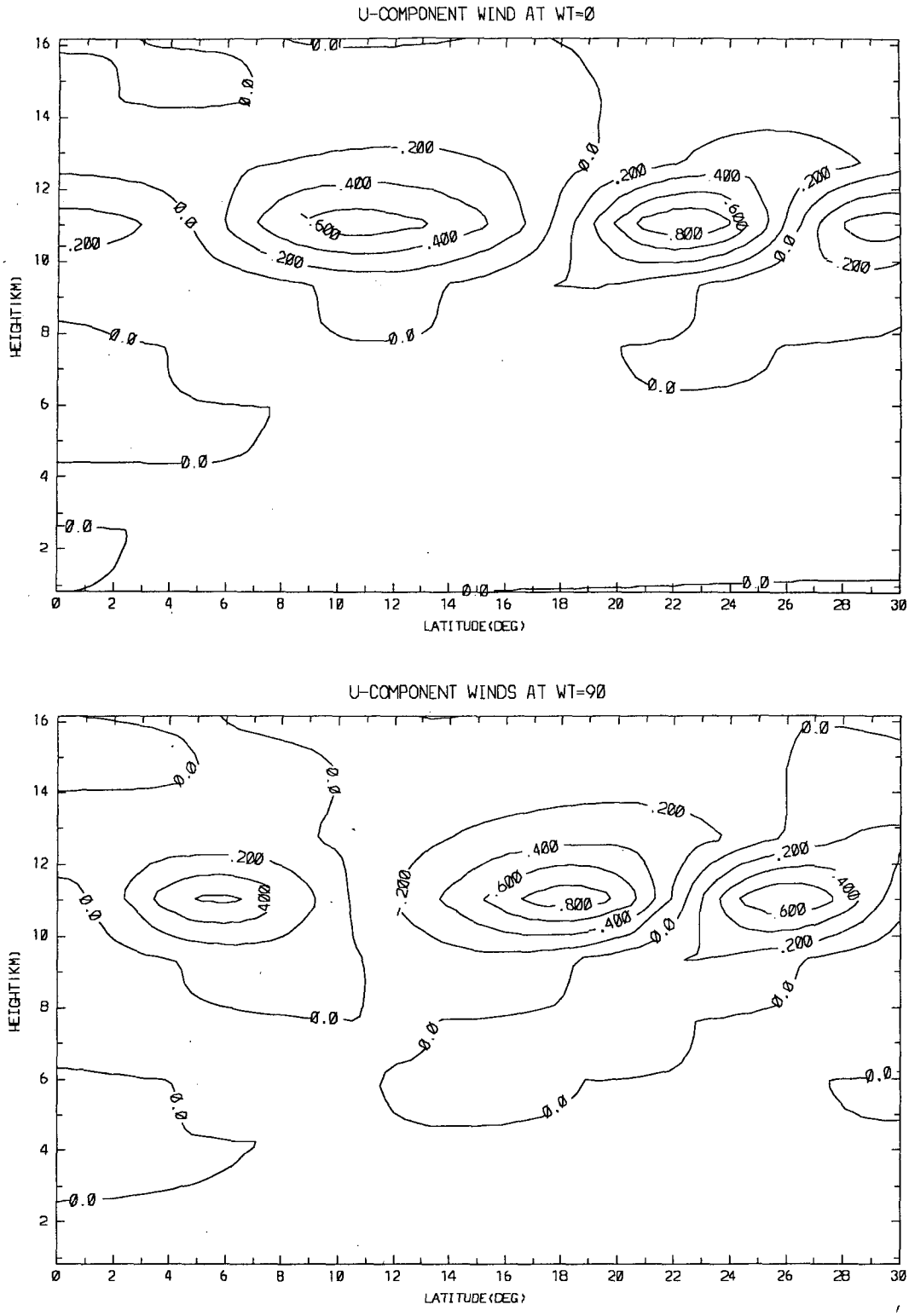

FIG. 5c. As in Fig. 5a, but mode depicted is associated with eigenvalue labeled (c) on Fig. 4.

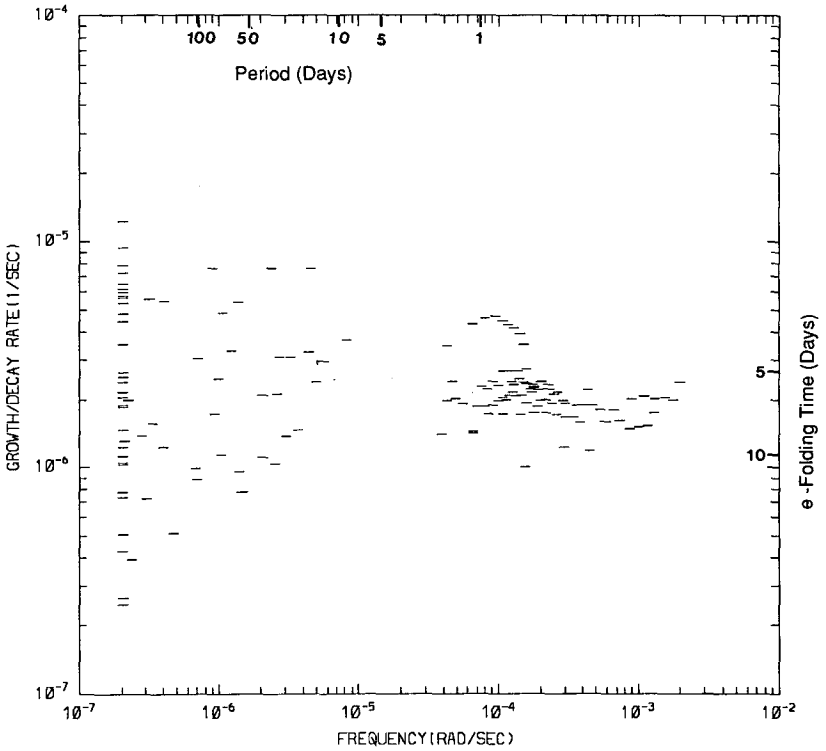

FIG. 6. As in Fig. 4, but with basic state cumulus mixing.

model variables must behave as a sum of damped complex exponentials whose frequencies are given by the eigenvalues as described previously.

The time series which we have chosen to illustrate the model state is an average of the upper tropospheric perturbation temperature for the region from 10°S to 10°N. An example of this series for a resting basic state calculation is shown in Fig. 7. This time series is presented for a run of 50 days duration, and shows the expected behavior consisting of a set of high-frequency inertia-gravity waves superimposed on an exponentially decaying thermal wind background state. Some of the very fastest (period < 1 day) inertia-gravity modes in the model have been damped by a time filter used for the model integration. The results of the same calculation for a Hadley cell basic state are presented in Fig. 8, and clearly show the tendency toward low-frequency oscillation. An analysis of the spatial fields associated with these runs show general agreement with our eigenvalue calculations in that the least-damped motions all exhibit the slow poleward propagation of an upper tropospheric zonal wind anomaly.

5. Discussion and conclusions

To summarize the results of the work described herein, we have shown that when the advective effects of a divergent Hadley type basic state are included in a linear model, zonally symmetric linear modes with natural oscillation frequencies in the 40–50 day range occur. The model modes in the general period range of 30–90 days appear to be the least damped modes in our model, so that one might expect that the continuous system would exhibit a tendency to oscillate at these time scales. This expectation has been confirmed by our experiments with a higher resolution prognostic calculation. A significant gap still remains in the use of this mechanism for a complete explanation of the oscillation time scale: namely, our present inability to explain the relationship between the linear slow modes and the modulation of cumulus convection. This effect undoubtedly plays a major role in the observed oscillation. We have performed similar calculations using the linear wave-CISK type cumulus parameterization scheme which is described in Stevens and Lindzen (1978). This scheme, which relates heating to low-level moisture convergence, has almost no effect on the nearly nondivergent slow model modes of the symmetric model.

It is our current working hypothesis that the changes in the convection are due to a modulation of the static stability of the tropical troposphere associated with the temperature fields of the slow modes. This hypothesis is mainly based on the results of calculations where we

have forced the zonally symmetric model with a prescribed time scale and noted that the model response is such that the model tropical static stability tends to be lower than average at the time of maximum heating. We are currently trying to investigate this effect in a model that is still simple enough to allow understanding of the model eigenmode structure. Additional support for this hypothesis has been given by the results of Goswami and Shukla (1983), who show that a fully nonlinear zonally symmetric general circulation model can exhibit slow oscillations similar to the ones discussed here. Goswami and Shukla have noted the tendency for the convection in their model to occur during periods of minimum moist static stability.

A second obvious obstacle to direct application of this work lies in our assumptions of zonal symmetry. Clearly, the observed oscillation is not zonally symmetric. At many times in the oscillation cycle the zonal wavenumber 1 component is as large or larger than the zonally symmetric one. A proper examination of this question requires the use of models with nonzonally symmetric basic states. At the time we began this work, the numerical solution of these models was beyond the capabilities of the then current computers and numerical techniques. We are now investigating the application of new methods and new computers to this problem and we hope to be able to remove this deficiency in the near future.

A second possibility for the nonzonally symmetric oscillation may be related to the traveling wave modes discussed by Chang (1977). It is possible that the observed oscillation may result from the combined effects of the zonally symmetric modes discussed here and the traveling modes, with the interaction between the two systems being accomplished by the modulation of West Pacific convection. In this sort of mechanism the zonally symmetric motions could provide a means of stabilizing the frequency of the wavenumber 1 traveling wave.

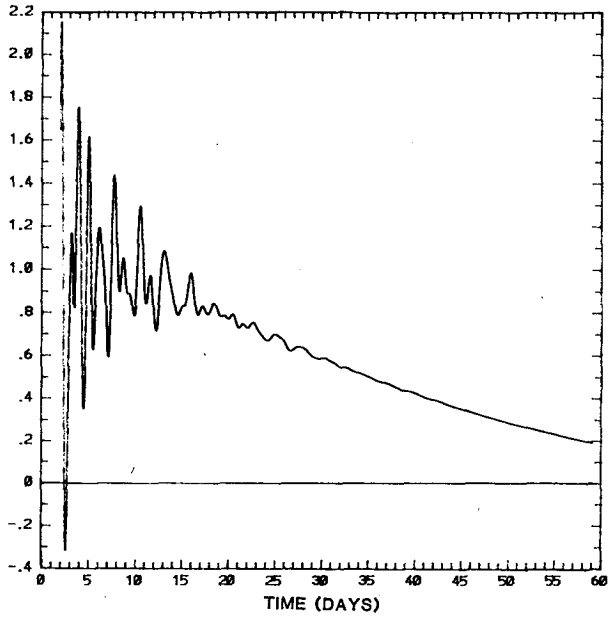

FIG. 7. Time series of temperature from upper troposphere of model (10°S to 10°N). Resting basic state.

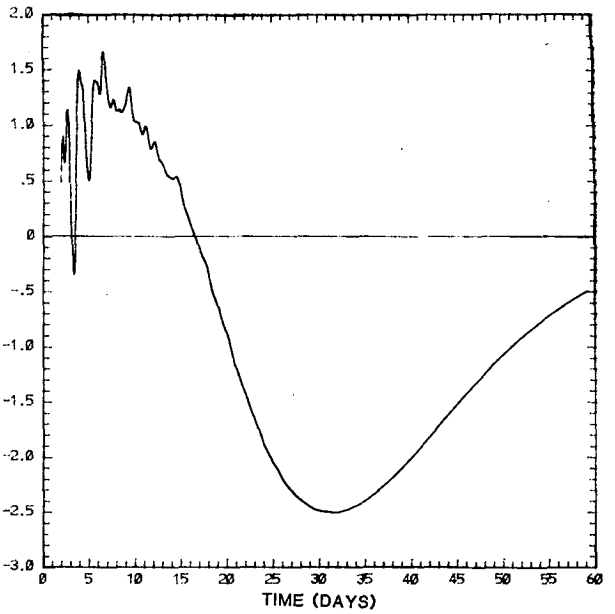

FIG. 8. As in Fig. 7, but for Hadley cell basic state.

It is our hope that the next few years will provide a convincing answer to the questions posed by this somewhat enigmatic phenomenon and that the work presented here will provide some insight into the possible physical and dynamical basis of the oscillation.

Acknowledgments. This work has been supported by NSF Grants ATM-8305759 and ATM-8405059 and NASA Grant NAG 5-136 to Colorado State University. The National Center for Atmospheric Research provided computing resources.

REFERENCES

Anderson, J. R., 1984: Slow motions in the tropical troposphere. Atmospheric Science Paper 381, Colorado State University, 144 pp.

——, and R. D. Rosen, 1983: The latitude–height structure of 40–50 day variations in atmospheric angular momentum. *J. Atmos. Sci.*, **40**, 1584–1591.

——, and D. E. Stevens, 1987: The response of the tropical atmosphere to slow thermal forcing. *J. Atmos. Sci.*, **44**, 676–686.

——, ——, and P. R. Julian, 1984: Temporal variation of the tropical 40–50 day oscillation. *Mon. Wea. Rev.*, **112**, 2431–2438.

Chang, C. P., 1977: Viscous internal gravity waves and low-frequency oscillations in the tropics. *J. Atmos. Sci.*, **38**, 2254–2364.

Gill, A. E., 1980: Some simple solutions for heat-induced tropical circulations. *Quart. J. Roy. Meteor. Soc.,* **106,** 447–462.

Goswami, B. N., and J. Shukla, 1984: Quasi-periodic oscillations in a symmetric general circulation model. *J. Atmos. Sci.,* **41,** 20–37.

Hoskins, B. J., and D. J. Karoly, 1981: The steady linear response of a spherical atmosphere to thermal and orographic forcing. *J. Atmos. Sci.,* **38,** 1179–1196.

Julian, P. R., and R. A. Madden, 1981: Ccomments on a paper by T. Yasunari. *J. Meteor. Soc. Japan,* **59,** 435–437.

Lindzen, R. S., 1967: Planetary waves on beta-planes. *Mon. Wea. Rev.,* **95,** 441–451.

Madden, R. A., and P. R. Julian, 1971: Detection of a 40–50 day oscillation in the zonal wind in the tropical Pacific. *J. Atmos. Sci.,* **28,** 702–708.

Matsuno, T., 1966: Quasi-geostrophic motions in the equatorial area. *J. Meteor. Soc. Japan,* **44,** 24–42.

Rosenlof, K. H., D. E. Stevens, J. R. Anderson and P. E. Ciesielski, 1986: The Walker circulation with observed zonal winds, a mean Hadley cell, and cumulus friction. *J. Atmos. Sci.,* **43,** 449–467.

Schneider, E. K., and R. S. Lindzen, 1976: A discussion of the parameterization of momentum exchange by cumulus convection. *J. Geophys. Res.,* **81,** 3158–3160.

Stevens, D. E., and R. S. Lindzen, 1978: Tropical wave-CISK with a moisture budget and cumulus friction. *J. Atmos. Sci.,* **35,** 940–961.

Yasunari, T., 1980: A quasi-stationary appearance of 30 to 40-day period in the cloudiness fluctuations during the summer monsoon over India. *J. Meteor. Soc. Japan,* **58,** 225–229.